

Differentially detected coherent population trapping resonances excited by orthogonally polarized laser fields

Michael Rosenbluh

Department of Physics, Bar-Ilan University, Ramat-Gan 52900, Israel

Vishal Shah and Svenja Knappe

Department of Physics, University of Colorado, Boulder, CO 80309

John Kitching

Time and Frequency Division, The National Institute of Standards and Technology, 325 Broadway, Boulder CO 80305

Abstract: We demonstrate the excitation and low-noise differential detection of a coherent population trapping (CPT) resonance with two modulated optical fields with orthogonal circular polarizations. When a microwave phase delay of $\lambda/4$ is introduced in the optical path of one of the fields, the difference in the power transmitted through the cell in each polarization shows a narrow, dispersive resonance. The differential detection allows a high degree of suppression of laser-induced noise and will enable nearly shot-noise-limited operation of atomic frequency references and magnetometers based on CPT.

© 2006 Optical Society of America

OCIS codes: 020.1670 (Coherent optical effects); 020.3690 (Line shapes and shifts); 270.1670 (Coherent optical effects)

References and Links

1. E. Arimondo, "Coherent population trapping in laser spectroscopy," *Prog. Opt.* **35**, 257-354 (1996).
2. S. E. Harris, "Electromagnetically induced transparency," *Phys. Today* **50**, 36-42 (1997).
3. G. Alzetta, A. Gozzini, L. Moi, and G. Orriols, "Experimental-Method for Observation of Rf Transitions and Laser Beat Resonances in Oriented Na Vapor," *Nuovo Cimento* **36**, 5-20 (1976).
4. E. Arimondo and G. Orriols, "Non-Absorbing Atomic Coherences by Coherent 2-Photon Transitions in a 3-Level Optical-Pumping," *Lett. Nuovo Cim.* **17**, 333-338 (1976).
5. S. J. Buckle, S. M. Barnett, P. L. Knight, M. A. Lauder, and D. T. Pegg, "Atomic Interferometers - phase dependence in multilevel atomic transitions," *Opt. Act.* **33**, 1129-1149 (1986).
6. D. Kosachiov, B. Matisov, and Y. Rozhdetsvensky, "Coherent Population Trapping - Sensitivity of an Atomic System to the Relative Phase of Exciting Fields," *Opt. Commun.* **85**, 209-212 (1991).
7. M. D. Lukin, S. F. Yelin, M. Fleishhauer, and M. O. Scully, "Quantum interference effects induced by interacting dark resonances," *Phys. Rev. A* **60**, 3225-3228 (1999).
8. W. Maichen, R. Gaggl, E. Korsunsky, and L. Windholz, "Observation of Phase-Dependent Coherent Population Trapping in Optically Closed Atomic Systems," *Europhys. Lett.* **31**, 189-194 (1995).
9. E. A. Korsunsky, N. Leinfellner, A. Huss, S. Balushev, and L. Windholz, "Phase-dependent electromagnetically induced transparency," *Phys. Rev. A* **59**, 2302-2305 (1999).
10. C. Affolderbach, S. Knappe, R. Wynands, A. V. Taichenachev, and V. I. Yudin, "Electromagnetically induced transparency and absorption in a standing wave," *Phys. Rev. A* **65**, 043810 (2002).
11. M. Zhu, Patent No. 6,359,916 (2002).
12. M. Stahler, R. Wynands, S. Knappe, J. Kitching, L. Hollberg, A. Taichenachev, and V. Yudin, "Coherent population trapping resonances in thermal Rb-85 vapor: D-1 versus D-2 line excitation," *Opt. Lett.* **27**, 1472-1474 (2002).
13. M. Zhu, "High contrast signal in a coherent population trapping based atomic frequency standard application," presented at the IEEE International Frequency Control Symposium and 17th European Frequency and Time Forum, Tampa, FL, 2003 (unpublished).
14. Y. Y. Jau, A. B. Post, N. N. Kuzma, A. M. Braun, M. V. Romalis, and W. Happer, "Intense, narrow atomic-clock resonances," *Phys. Rev. Lett.* **92**, 110801 (2004).

15. S. V. Kargapol'tsev, J. Kitching, L. Hollberg, A. V. Taichenachev, V. L. Velichansky, and V. I. Yudin, "High-contrast dark resonance in $\sigma(+)$ - $\sigma(-)$ optical field," *Laser Phys. Lett* **1**, 495-499 (2004).
16. Y. Y. Jau, E. Miron, A. B. Post, N. N. Kuzma, and W. Happer, "Push-pull optical pumping of pure superposition states," *Phys. Rev. Lett.* **93**, 160802 (2004).
17. A. B. Post, Y. Y. Jau, N. N. Kuzma, and W. Happer, "Amplitude- versus frequency-modulated pumping light for coherent population trapping resonances at high buffer-gas pressure," *Phys. Rev. A* **72**, 033417 (2005).
18. T. Zanon, S. Guerandel, E. de Clercq, D. Holleville, N. Dimarcq, and A. Clairon, "High contrast Ramsey fringes with coherent-population-trapping pulses in a double lambda atomic system," *Phys. Rev. Lett.* **94**, 193002 (2005).
19. A. V. Taichenachev, V. I. Yudin, V. L. Velichansky, and S. A. Zibrov, "On the unique possibility of significantly increasing the contrast of dark resonances on the D1 line of Rb-87," *JETP Letters* **82**, 398-403 (2005).
20. J. Kitching, S. Knappe, N. Vukicevic, L. Hollberg, R. Wynands, and W. Weidmann, "A microwave frequency reference based on VCSEL-driven dark line resonances in Cs vapor," *IEEE Trans. Instrum. Meas.* **49**, 1313-1317 (2000).
21. J. Vanier, "Atomic clocks based on coherent population trapping: a review," *Appl. Phys. B* **81**, 421-442 (2005).
22. T. Haslwanter, H. Ritsch, J. Cooper, and P. Zoller, "Laser-Noise-Induced Population Fluctuations in 2-Level and 3-Level Systems," *Phys. Rev. A* **38**, 5652-5659 (1988).
23. J. C. Camparo, "Conversion of laser phase noise to amplitude noise in an optically thick vapor," *J. Opt. Soc. Am. B* **15**, 1177-1186 (1998).
24. S. Knappe, V. Shah, P. D. D. Schwindt, L. Hollberg, J. Kitching, L. A. Liew, and J. Moreland, "A microfabricated atomic clock," *Appl. Phys. Lett.* **85**, 1460-1462 (2004).
25. A. Nagel, L. Graf, A. Naumov, E. Mariotti, V. Biancalana, D. Meschede, and R. Wynands, "Experimental realization of coherent dark-state magnetometers," *Europhys. Lett.* **44**, 31-36 (1998).
26. P. D. D. Schwindt, S. Knappe, V. Shah, L. Hollberg, J. Kitching, L. A. Liew, and J. Moreland, "Chip-scale atomic magnetometer," *Appl. Phys. Lett.* **85**, 6409-6411 (2004).
27. A. F. Huss, R. Lammegger, C. Neureiter, E. A. Korsunsky, and L. Windholz, "Phase correlation of laser waves with arbitrary frequency spacing," *Phys. Rev. Lett.* **93**, 223601 (2004).
28. H. Goldstein, *Classical Mechanics*, 2nd ed. (Addison-Wesley, Reading, MA, 1980).

1. Introduction

Coherent population trapping (CPT) [1], like the associated phenomenon of electromagnetically induced transparency (EIT) [2], is based on the creation of coherences in an atomic medium with optical fields and the resulting modification of the medium's optical susceptibility. The simplest demonstration of coherent population trapping between hyperfine-split levels of atoms was described in Refs. [3,4]. In these experiments, two circularly polarized light fields separated in frequency by the atom's hyperfine splitting generated the coherence in a thermal vapor of alkali atoms. Since then, more complex excitation schemes have been implemented. For example, double- Λ systems with closed optical excitation paths [5-7] have been investigated in the context of optical switching [8,9]. In addition, CPT in a standing wave geometry was investigated both experimentally and theoretically in Ref. [10]. A substantial body of work has also been carried out with the goal of enhancing the amplitude of CPT resonances [11-19] for application to atomic frequency references and magnetometers.

The noise processes that affect the measurement of CPT resonances have also been studied in detail [20,21]. These include photon and atom shot noise, frequency and excess amplitude noise on the excitation laser [22,23], and electronic noise. These noise processes put practical and fundamental limits on the performance of devices based on CPT resonances, such as atomic clocks [21,24] and magnetometers [25,26], particularly in the case of compact systems using diode lasers. In this letter, we report the observation of a CPT resonance using differential detection of two co-propagating excitation beams with orthogonal polarizations. This work builds on the push-pull optical pumping work by Jau, *et al.* [16] and pulsed CPT work of Zanon, *et al.* [18], and in principle offers the same advantage of high signal contrast. However, here we gain the additional benefit that most noise processes are strongly suppressed by the differential nature of the resonance detection; we observe a reduction of the noise power spectral density at low frequencies by two orders of magnitude under optimal conditions to within a factor of two of the fundamental shot noise limit.

2. Experimental setup

The experimental configuration is shown in Fig. 1(a). A linearly polarized laser field is generated by a vertical cavity surface emitting laser (VCSEL) tuned to the D1 transition in ^{87}Rb at 795 nm. The laser injection current is modulated at a frequency equal to one-half the atomic hyperfine splitting frequency of 6.8 GHz. This creates two first-order sidebands on the optical carrier that are suitable for exciting a CPT resonance in the atoms. The laser output is collimated and separated into two orthogonally polarized beams of roughly equal intensity, by using a combination of a half-wave plate and polarizing beam splitter. A polarizer, placed before the half-wave plate and oriented to transmit most of the laser light, prevents polarization fluctuations from generating anti-correlated noise in the two orthogonally polarized beams. One beam is delayed by propagation through several centimeters of air, and the beams are recombined with a second polarizing beam splitter. The combined beams pass through a quarter-wave plate oriented to transform the linear polarizations into circular polarizations, then enter an alkali vapor cell (CPT cell) containing isotopically enriched ^{87}Rb and N_2 at a pressure of 1.3 kPa. The vapor cell is a cuboid of volume 4.5 cm^3 , and is shielded from external magnetic fields by a high permeability enclosure. A longitudinal magnetic field of $30\text{ }\mu\text{T}$ is applied inside the shield to lift the degeneracy of the Zeeman sub-levels. The atoms in the cell therefore see two pairs of CPT fields with orthogonal polarizations. The relative phase of the optical difference frequency can be adjusted by varying the propagation delay. The laser detunings and polarizations with respect to the atomic levels are illustrated in Fig. 1(b).

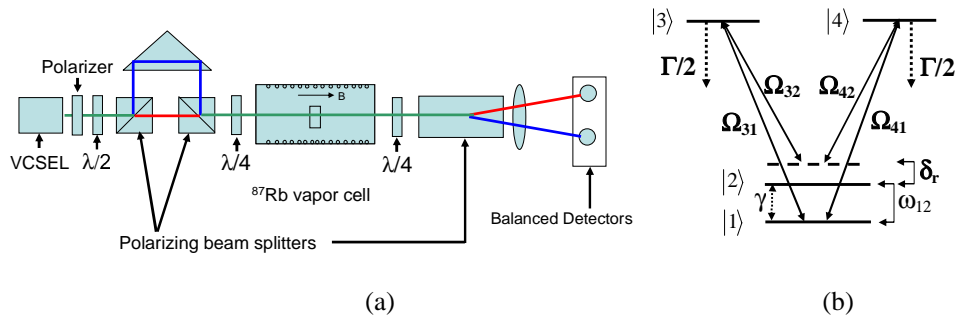


Fig. 1. (a) Experimental configuration for differential detection of CPT resonances. (b) Atomic level diagram showing detunings and polarizations of the incident optical fields. Here Ω_{ij} is the Rabi frequency connecting levels i and j , $\Gamma/2$ is the population decay rate from the excited states to each hyperfine state and γ is the decay rate of the hyperfine coherence. The optical fields are assumed to be on resonance and δ_r is the Raman detuning.

The laser frequency is locked to an absorption signal from a separate reference cell containing no buffer gas such that the two first-order sidebands on the optical carrier are resonant with the $5S_{1/2}, F=1 \rightarrow 5P_{1/2}, F=2$ and $5S_{1/2}, F=2 \rightarrow 5P_{1/2}, F=2$ transitions in the Rb vapor cell. The temperature of the CPT cell is maintained near $35\text{ }^\circ\text{C}$ such that $\sim 75\%$ of the resonant optical power incident on the cell is absorbed under the conditions described above. The beam diameter is set with an aperture to 2.5 mm, and the total optical power in both beams entering the CPT cell is $33\text{ }\mu\text{W}$. After exiting the cell, the beams pass through a second quarter-wave plate, which restores the beams to their original linear polarizations. A polarizing beam splitter separates the two polarizations, which are then focused onto two balanced photodetectors; the signals from the photodetectors can be added, subtracted, or measured individually, as needed.

When the delayed beam is blocked, a standard CPT configuration results [3]. The power transmitted through the cell is measured as a function of the frequency of the laser modulation signal as it is scanned near 3.417,344,417 GHz. A CPT resonance, associated with the $F=1, m_F=0 \rightarrow F=2, m_F=0$ transition, of width 600 Hz (at 3.4 GHz) is measured, as shown in Fig. 2(a). The delayed beam is then unblocked and the delay length is set to 11.6 mm,

approximately equal to $\lambda_{\text{mw}}/4$, where λ_{mw} is equal to the wavelength of the 6.8 GHz hyperfine splitting frequency (44 mm). The signals from the balanced detectors are then subtracted and the resulting signal is shown in Fig. 2(b). The signal is dispersive in nature, has roughly the same width and amplitude as the single-beam CPT resonance, and has considerably less noise. Fig. 2(c) and Fig. 2(d) show the signals from each photodetector individually when both beams propagate in the cell. It is clear that the presence of a second beam with an orthogonal polarization creates an asymmetry in the line shape of the first beam. This asymmetry depends on whether the phase of the second beam is delayed or advanced with respect to the first. Similar asymmetrical CPT resonance lineshapes have been observed previously in a standing-wave geometry [10] but were attributed to detuning of the optical field from the atomic resonance.

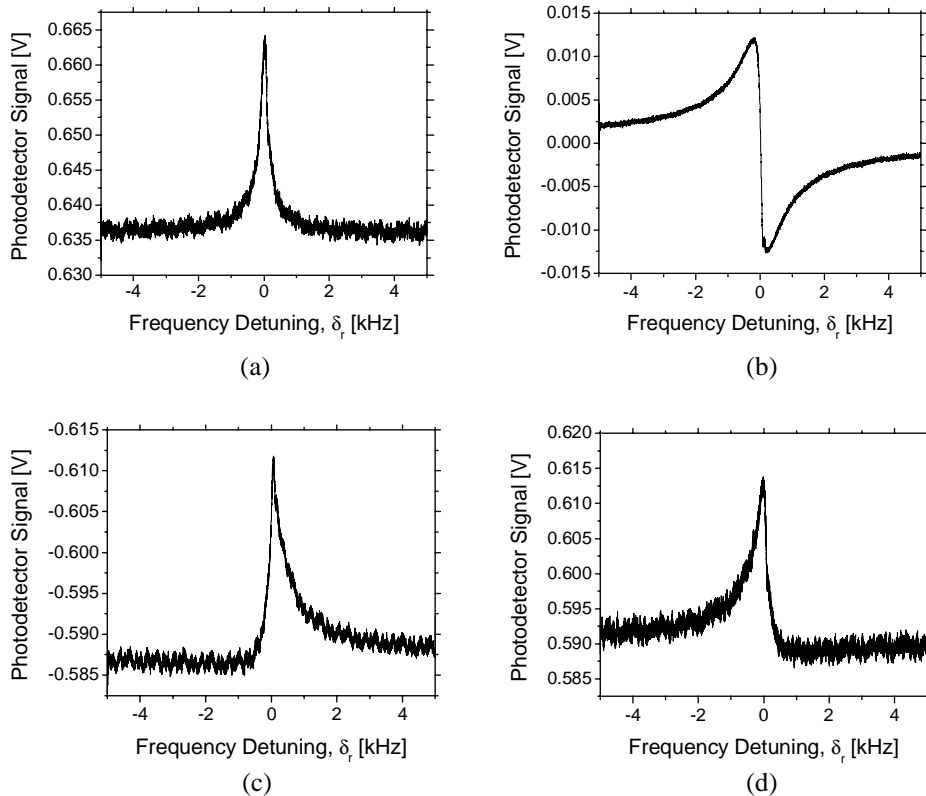


Fig. 2. Lineshapes of atomic-coherence-induced resonances for phase-shifted, two-beam excitation. (a) One beam blocked, conventional CPT resonance, (b) both beams present, signals from balanced photodetectors subtracted, (c) both beams present, phase-advanced signal only, (d) both beams present, phase-delayed signal only.

The noise suppression evident in Fig. 2(b) was quantified by measuring the low-frequency noise spectrum with an FFT spectrum analyzer (Fig. 3). Noise suppression of about 20 dB is observed for the difference signal for both the coherent signals (generated predominantly by noise from the 60 Hz line signal) and broadband noise. This noise suppression would be expected to improve the frequency stability of a reference or the sensitivity of a magnetometer by a factor of 10, and is within a factor of two of the shot noise limit for the optical power levels used if the background electronic noise is subtracted. The differential technique we describe here should be superior to a conventional differential detection scheme, in which the optical power before the cell is subtracted from the CPT signal measured after the cell. This is because the scheme described here in principle suppresses noise due to both power and

frequency fluctuations of the laser, whereas conventional differential detection suppresses only power fluctuations.

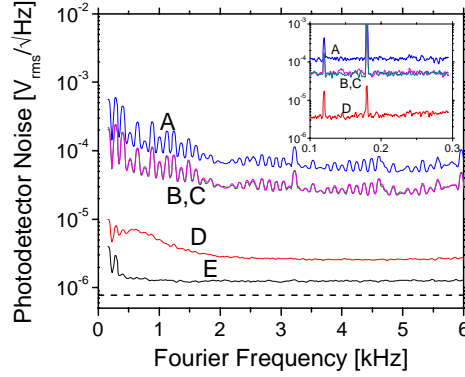


Fig. 3. Noise spectra taken with the local oscillator tuned to resonance with the center of the CPT transition ($\delta_r = 0$). Trace A is the sum of the balanced detector channels, Traces B and C are the phase advanced and delayed detector channel respectively, Trace D is the difference of the channels and Trace E is the electronic noise floor (both beams blocked). The inset shows a smaller frequency range and the white noise component of the spectrum around 200 Hz. The dashed line indicates the approximate shot noise level for the sum and difference configurations, as estimated from the DC detector photocurrents.

3. Theoretical analysis

We interpret the experimental results through a density matrix analysis of the four-level model shown in Fig. 1(b). For simplicity, we assume the Rabi frequencies are all equal in magnitude, and we set the phases of the incident light fields such that $\Omega_{31} = \Omega/2$, $\Omega_{32} = e^{-i\theta}\Omega/2$, $\Omega_{41} = \Omega e^{i\theta}/2$ and $\Omega_{42} = e^{i\theta}\Omega e^{i\theta}/2$. This parameterization ignores the overall phase of the light fields and assumes that both sets of sidebands are generated by the same modulation source. Since the $m_F = 0 \rightarrow m_F = 0$ coherence can be excited only by pairs of optical fields with the same polarization state, and the $m_F = \pm 1 \rightarrow m_F = \mp 1$ coherences are not dark for the $F=2 \rightarrow F'=2$ transition, the atomic dynamics are independent of the relative optical phase between the two CPT fields, θ . This parameter can therefore be set to zero without compromising the applicability of the model to the experimental configuration.

We solve the density matrix equation of motion under steady-state conditions, $d\rho/dt = 0$, and obtain expressions for the atomic ground state coherence and the absorption of the individual light fields:

$$\rho_{12} = -\frac{\Psi \cos(\phi)}{\gamma + 2\Psi + i\delta_r} \quad (1)$$

$$\text{Im}[\Omega_{i4}^* \rho_{i4}] = \Psi - \frac{2(\gamma + 2\Psi)\Psi^2 \cos^2(\phi)}{\delta_r^2 + (\gamma + 2\Psi)^2} - \frac{\delta_r \Psi^2 \sin(2\phi)}{\delta_r^2 + (\gamma + 2\Psi)^2} \quad (2a)$$

$$\text{Im}[\Omega_{i3}^* \rho_{i3}] = \Psi - \frac{2(\gamma + 2\Psi)\Psi^2 \cos^2(\phi)}{\delta_r^2 + (\gamma + 2\Psi)^2} + \frac{\delta_r \Psi^2 \sin(2\phi)}{\delta_r^2 + (\gamma + 2\Psi)^2} \quad (2b)$$

where $\Psi = |\Omega|^2 / 2\Gamma$. We see that Eq. (2a) and Eq. (2b) contain both an absorptive term (the second term) and a dispersive term (the third term). The expressions (2a) and (2b) are closely

related to the analysis in Ref. [27], where an expression for the phase noise transfer coefficient is derived for optical fields in a double- Λ system. The individual resonances of Eq. (2) are plotted in Fig. 4. Good qualitative agreement is observed between the theoretical results for $\phi = \pi/4$ and the experimental data shown in Fig. 2(c) and Fig. 2(d). Equations (2a) and (2b) also qualitatively explain the noise suppression evident in Fig. 3. When these expressions are subtracted, as is the case when differential detection is used, the resulting expression has a second-order dependence on the normalized laser intensity Ψ , rather than the first-order dependence of each expression individually. This second-order dependence is responsible for the suppression of laser intensity noise in the differentially detected signal.

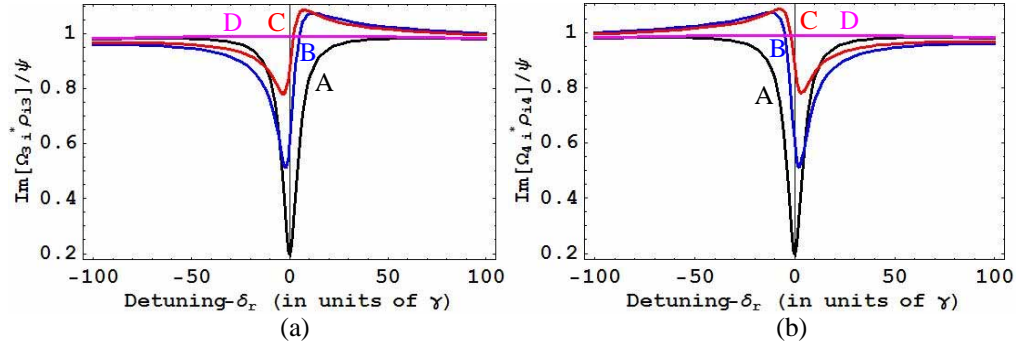


Fig. 4. Calculated resonance lineshapes for the model in Fig. 1(b) for $\Psi/\gamma = 1$. Fractional absorption for the (a) phase-delayed and (b) phase-advanced field as a function of Raman detuning. Trace A: $\phi = 0$; Trace B: $\phi = \pi/4$; Trace C: $\phi = 3\pi/8$; Trace D: $\phi = \pi/2$. These results for $\phi = \pi/4$ correspond closely to the experimental data shown in Fig. 2(c) and (d).

If the resonance of Fig. 2(b) is used to stabilize the frequency of an externally applied signal from a local oscillator, it is important to consider frequency shifts and drifts related to this differential method of excitation and detection. In particular, we consider the effects of both power asymmetry between the two laser beams and imperfect phase adjustment ($\phi \neq \pi/4$) on the resonance zero crossing. We estimate this by re-evaluating Eq. 2a and Eq. 2b for small asymmetry in Rabi frequency of the two polarizations, $\Delta\Omega$, and small phase deviation $\Delta\phi$ from $\pi/4$. We note that the shift due to the overall DC signal change can be eliminated through the use of modulation and second harmonic detection, and find that the frequency shift under these conditions to first order in $\Delta\Omega$ and $\Delta\phi$ is given by

$$\beta = \frac{\Omega^2}{2(\gamma\Gamma + \Omega^2)} \frac{\Delta\Omega}{\Omega} \gamma. \quad (3)$$

Thus, a power stability of $\sim 0.1\%$ would be required to maintain a fractional frequency shift below 10^{-11} for a transition linewidth of 100 Hz. The frequency shift is first-order insensitive to the microwave phase delay when $\Delta\Omega \neq 0$ and insensitive to all orders when $\Delta\Omega = 0$.

4. Interpretation

To interpret these results we consider a simple harmonic oscillator (SHO) [28] with generalized position ρ , resonant frequency ω_{12} and damping constant γ , interacting with two sinusoidally varying driving fields at the same frequency but with different phases: $F_1(t) = \Omega e^{i(\omega_L t + \phi)}$ and $F_2(t) = \Omega e^{i(\omega_L t - \phi)}$. Solving this system under steady-state conditions in the rotating frame, and under the assumption that $\delta \ll \omega_{12}$ ($\delta \equiv \omega_L - \omega_{12}$), we find that the average generalized power absorbed by the oscillator from each driving field is given by

$$\langle \text{Im}[F_1^* \rho] \rangle = \frac{2\gamma(\Omega^2 / 2\omega_{12})\cos^2(\phi)}{\delta^2 + \gamma^2} + \frac{\delta(\Omega^2 / 2\omega_{12})\sin(2\phi)}{\delta^2 + \gamma^2} \quad (4a)$$

$$\langle \text{Im}[F_2^* \rho] \rangle = \frac{2\gamma(\Omega^2 / 2\omega_{12})\cos^2(\phi)}{\delta^2 + \gamma^2} - \frac{\delta(\Omega^2 / 2\omega_{12})\sin(2\phi)}{\delta^2 + \gamma^2} \quad (4b)$$

By comparing Eq. (4) to Eq. (2) we can see that energy absorption in the SHO with a two-phase driving field has the same spectral character as light absorption in a double- Λ CPT system.

In the case analyzed here, where the two driving fields are of equal strength, the atomic coherence that is excited has a phase that is equal to the mean of the phases of the individual driving fields and an amplitude proportional to the cosine of one-half the phase difference between the driving fields. As the phase of one driving field is changed with respect to the other, there are therefore two separate parameters that determine the absorption spectrum of the fields. The first is the amplitude of the atomic coherence generated by the fields, which is determined by the phase of one driving field with respect to the other. The second is the difference between the phases of the atomic coherence and each of the individual fields. As in any phase-sensitive receiver, the magnitude of this phase difference determines the relative magnitudes of the absorptive-like and dispersive-like components of the resonance spectrum and the sign of this phase determines the sign of the asymmetry. For example, when the driving fields are exactly out of phase ($2\phi = \pi$), no atomic coherence is generated, and therefore no resonance exists. However, the small coherence created when this relative phase is slightly different from π produces a predominantly dispersive-like absorption profile for each driving field. On the other hand, when the two driving fields are exactly in phase ($2\phi = 0$), a large atomic coherence is generated that is exactly in phase with both driving fields, and a strong absorptive-like resonance is observed in both field absorption spectra [16,18]. In the intermediate case ($2\phi = \pi/2$), a moderately large coherence is generated that is out of phase by $\pi/4$ from each driving field. In this case the coherence generates absorption spectra in each field composed of equal parts absorptive-like and dispersive-like components. These spectra are shown in Fig. 2(c) and 2(d).

In conclusion, we demonstrate that by measuring the difference in transmitted power in two orthogonally polarized pairs of CPT fields incident simultaneously on a collection of atoms we achieve a substantial reduction in the noise with almost no loss of signal amplitude or broadening of signal width. This allows observation of CPT-like resonances connected with the coherences excited in the atomic sample with almost no noise contamination from laser-related sources and results in near-shot-noise-limited resolution. In addition, the use of two orthogonal circular polarizations prevents the loss of atomic population to the extreme magnetic sublevels ($m_F = \pm F$) that can occur when only one circularly polarized laser field is present and excitation occurs on the D1 line [15,16], and therefore improves the signal amplitude. Low noise detection of atomic coherences is not only interesting from a spectroscopic point of view, but also may result in significant improvements of devices based on CPT such as atomic clocks and magnetometers. The measurements can be readily understood with a simple, four-level model and can be interpreted as a simple harmonic oscillator interacting with two driving fields with a relative phase shift.

Acknowledgments

The authors gratefully acknowledge valuable advice from L. Hollberg, useful discussions with A. V. Taichenachev and V. I. Yudin regarding the theoretical analysis, and experimental help from P.D.D Schwindt and V. Gerginov. This work was supported by the Microsystems Technology Office of the U.S. Defense Advanced Research Projects Agency (DARPA). This work is a contribution of NIST, an agency of the U.S. government, and is not subject to copyright.